Acta Cryst. (1996). B52, 131–139

Single-Crystal Structure Analysis and Energy Minimizations of a MFI-Type Zeolite at Low *p*-Dichlorobenzene Sorbate Loading

H. VAN KONINGSVELD,[a] J. C. JANSEN[a] AND A. J. M. DE MAN[b]

[a]*Laboratories of Applied Physics and Organic Chemistry and Catalysis, Lorentzweg 1, 2628 CJ Delft, The Netherlands, and* [b]*Arbeitsgruppe Quantenchemie an der Humboldt-Universität, Max-Planck-Gesellschaft, Jaegerstrasse 10/11, D-10117 Berlin, Germany*

(*Received 19 September 1994; accepted 23 June 1995*)

Abstract

The crystal structure of a low-loaded adsorption complex of H-ZSM-5 with *p*-dichlorobenzene has been studied by single-crystal X-ray diffraction. The controversy in the literature, concerning the preferred location of the *p*-dichlorobenzene molecule, is explained by different interpretations of the difference electron-density map representing the electron density of the adsorbed molecule. The crystal studied contains 2.56(2) *p*-dichlorobenzene molecules per unit cell. The adsorbed molecules prefer the position at the intersection of channels. Energy calculations, using the Biosym Catalysis and Sorption Software, strongly support this interpretation. In nearly all calculations the orientation of the relaxed molecule is close to the orientation found from the X-ray analysis. A second rotational position at the intersection, suggested from calculations in a fully relaxed structure, resembles the location of the *p*-xylene molecule at the intersection of channels in the high-loaded H-ZSM-5/8*p*-xylene complex. The unit cell of $Si_{11.96}Al_{0.04}O_{24}.0.32C_6H_4Cl_2(+0.04H^+)$, $M_r = 767.42$, is orthorhombic, *Pnma*, with $a = 20.009(3)$, $b = 19.909(4)$, $c = 13.366(2)$ Å, $V = 5324(2)$ Å^3, $Z = 8$, $D_x = 1.922$ Mg m^{-3} and μ(Mo $K\alpha$) = 0.734 mm^{-1}. The final $R(wR)$ is 0.044 (0.048), $w = 1/\sigma^2(F)$, for 5306 observed reflections with $I > 2.0\sigma(I)$ measured at 293 K.

1. Introduction

MFI-type zeolites can be built from a building unit containing 12 *T* atoms (*T* = Si, Al) connected through 26 O atoms. O atoms are approximately between *T* atoms. The MFI framework can be generated by applying simple symmetry operations to this T_{12}-building unit (van Koningsveld, Tuinstra, van Bekkum & Jansen, 1989). The MFI-type zeolites display an intersecting two-channel system, which has a bearing on the dynamics and equilibrium of adsorption. H-ZSM-5 is a MFI-type zeolite, in which a varying number of Si atoms is replaced by Al atoms. The negative charge introduced into the framework by aluminum is compensated for by H ions. In H-ZSM-5, fully loaded with *p*-xylene [eight molecules per unit cell (u.c.)], the adsorbate was found to be orderly located, allowing its packing determination by X-ray analysis (van Koningsveld *et al.*, 1989).

The equilibrium location of *p*-dichlorobenzene (pdcb) in H-ZSM-5 has been studied by several authors. Gies, Marler, Fyfe, Kokotailo, Feng & Cox (1991) concluded from Rietveld refinement of synchrotron powder data that in a low-loaded H-ZSM-5 complex (2 pdcb/u.c.) the pdcb molecules are located in the straight channel section and not at the intersection of the straight and sinusoidal channels, where part of the homomorphous *p*-xylene molecules in a high-loaded H-ZSM-5/*p*-xylene complex (van Koningsveld *et al.*, 1989) are located. This implies a shift of the pdcb molecules over $\frac{1}{4}\mathbf{b}$ away from the intersection. van Koningsveld, Jansen & van Bekkum (1992) arrived at the same conclusion using X-ray data from what they believed to be a single crystal of a maximal-loaded H-ZSM-5/pdcb complex. Finally, Mentzen & Sacerdote-Peronnet (1993) reported on the structures of low- (4 pdcb/u.c.) and high-(>4 pdcb/u.c.) loaded H-ZSM-5/pdcb complexes determined by X-ray powder diffraction. According to these authors pdcb molecules are present at the intersection of channels at all loadings. The symmetry is *Pnma* up to loadings of four pdcb molecules per unit cell. The authors showed that the structural details of the high-loaded complex are comparable to those observed in the high-loaded H-ZSM-5/*p*-xylene complex (van Koningsveld *et al.*, 1989): the symmetry changes to $P2_12_12_1$ and four additional pdcb molecules are present in the sinusoidal channels.

Different interpretations of the electron-density map might have led to these apparently conflicting results with respect to the location of the pdcb molecules. As was suggested by Mentzen & Sacerdote-Peronnet (1993), domains might have been present in the earlier studied complexes. These domains, corresponding to high- and low-loaded regions, exhibiting different symmetries in the crystals, might have obscured the observations. To avoid these complications, a low-loaded single crystal of H-ZSM-5 with pdcb was prepared. X-ray diffraction was used to study the actual structure of the complex. Energy

calculations were carried out to obtain additional information on the preferred adsorption site(s) within the H-ZSM-5 framework.

2. Experimental

Calcined H-ZSM-5, prepared according to a procedure described by van Koningsveld, Jansen & van Bekkum (1987), Si/Al $\approx$ 300, was exposed in a closed vessel to a saturated vapour of pdcb at 350 K over 2 h. Subsequently, the crystals were cooled down by 3 K min^{-1}. The crystal selected for X-ray analysis measured 0.20 × 0.15 × 0.25 mm in the *a*, *b* and *c* directions, respectively, and was mounted along the *c* axis on an Enraf–Nonius CAD-4 diffractometer. Lattice constants were determined from 25 reflections with $10 < \theta < 17°$. Data were collected to $\theta_{max} = 30.0°$ (h 0 → 28, k 0 → 28, l 0 → 18) using the $\omega/2\theta$ scan, width = $(0.85 + 0.35 \tan\theta)°$, requesting $\sigma_{count}(I)/I < 0.02$ in a scan or with a maximum recording time of 120 s. Intensities of 7936 reflections were measured with graphite-monochromated Mo $K\alpha$ radiation (λ = 0.71073 Å), of which 5309 reflections with $I > 2.0\sigma(I)$ were used. Three reference reflections were measured every 2 h of X-ray measuring time; the observed intensity decay of 9.5%, due to instability of the primary beam, was accounted for. See Table 1 for full experimental details. The initial positions of the framework atoms were taken from the literature (van Koningsveld, 1990). All *T* atoms (Si, Al) were treated as zero-valent Si. Anisotropic refinement on *F* in *Pnma* converged to $R(wR) = 0.063$ (0.119), with $w = 1/\sigma^2(F)$. The difference electron-density map, calculated at this stage of the refinement, could be interpreted in two almost equally probable ways. These two models are discussed in the next section (Fig. 1). The preferred Model II, with a disordered pdcb molecule around *m*, refined to $R = 0.044$, $wR = 0.048$ [$w = 1/\sigma^2(F)$] and $S = 2.99$ for 5306 observed reflections and 356 parameters. The population of the pdcb molecule refines to 0.320 (3), which corresponds to 2.56 (2) molecules per unit cell. Three low-order reflections, possibly affected by extinction, were left out of the final refinement cycles. The average and maximum shift/e.s.d. were 0.002 and 0.034 [y(Cl(2))], respectively. In the final difference-Fourier synthesis the three highest peaks ($0.83 < \Delta\rho < 1.14$ e Å^{-3}) could be attributed to rest densities of framework O atoms. There is some rest density at the pdcb position (~ 0.7 e Å^{-3}). All other peaks (< 0.7 e Å^{-3}) were in close vicinity of the framework atoms. No absorption or extinction corrections were applied. All calculations were performed on a SUN-IPX workstation using the programs of the *Xtal*3.2 system (Hall, Flack & Stewart, 1992). Energy calculations for various possible adsorption sites were carried out on a Silicon Graphics Iris Indigo workstation using the software program *Discover*-3 (Biosym Technologies, 1993).

Table 1. *Experimental details*

Crystal data	
Chemical formula	$Si_{11.96}Al_{0.04}O_{24}.0.32C_6H_2Cl_2$
Chemical formula weight	767.42
Cell setting	Orthorhombic
Space group	*Pnma*
a (Å)	20.009 (3)
b (Å)	19.909 (4)
c (Å)	13.366 (2)
V (Å^3)	5324 (2)
Z	8
D_x (Mg m^{-3})	1.922
Radiation type	Mo $K\alpha$
Wavelength (Å)	0.71073
No. of reflections for cell parameters	25
θ range (°)	10–17
μ (mm^{-1})	0.734
Temperature (K)	298
Crystal form	Block
Crystal size (mm)	0.15 × 0.20 × 0.25
Crystal colour	Yellowish
Data collection	
Diffractometer	Enraf–Nonius CAD-4
Data collection method	ω 2θ
Absorption correction	None
No. of measured reflections	7936
No. of independent reflections	5309
No. of observed reflections	5306
Criterion for observed reflections	$I > 2\sigma(I)$
R_{int}	Not calculated
θ_{max} (°)	30
Range of h, k, l	0 → h → 28 0 → k → 28 0 → l → 18
No. of standard reflections	3
Frequency of standard reflections	Every 2 h
Intensity decay (%)	9.5
Refinement	
Refinement on	F
R	0.044
wR	0.048
S	2.99
No. of reflections used in refinement	5306
No. of parameters used	356
Weighting scheme	$w = 1\sigma^2(F)$
$(\Delta/\sigma)_{max}$	0.034
$\Delta\rho_{max}$ (e Å^{-3})	1.14
$\Delta\rho_{min}$ (e Å^{-3})	0.83
Extinction method	None

3. Results and discussion

3.1. *X-ray diffraction*

Fig. 1 shows the difference electron-density map at the stage of refinement where $wR = 0.119$ (see *Experimental*). The maxima in the map are numbered 1–4. A geometrical analysis of the peaks gives two possible models for the intramolecular chlorine–chlorine vector of pdcb (= 6.243 Å; Wheeler & Colson, 1975). The Cl—Cl vector can be disordered between peaks 1 and 2 [Cl(1)—Cl(2a) $\approx$ 6.14 Å] and 1′ and 3 (or 4), where 1′ is 1 repeated by $\bar{1}$. The average distance between 1′ and 3 and 1′ and 4, Cl(1)—Cl(2b), is $\sim$ 6.11 Å. This (disordered) possibility is labelled Model I (*a* and *b*, respectively).

In Model II the Cl—Cl vector is ascribed to peaks 1 and 1″ [Cl(1)—Cl(1″) ≈ 6.22 Å], where the double prime indicates the *m*-related position. The pdcb molecule in I is shifted with respect to the molecule in II over $\frac{1}{4}\mathbf{b}$: in I the pdcb molecule is in the straight channel and in II the molecule is at the intersection of channels or, in other words, approximately around $\bar{1}$ and *m*, respectively. No C atoms can be detected in I. In II peaks 2–4 are assigned to C atoms. Refinement of both models, without any constraints on the atoms, gives the same *wR* factor. Relevant data are summarized in Table 2. The final geometry is unrealistic for both models. In Model I the Cl(1)—Cl(2*a*) and Cl(1)—Cl(2*b*) distances are 6.16(2) and 6.36(2), respectively, whereas in Model II the two C—C distances across *m* are 1.37(2) and 1.46(3) Å, with C—C(Cl)—C = 134(2)°. Restrained refinement of I, using Cl—Cl = 6.243(5), increases the *wR* factor slightly to *wR* = 0.054, whereas refinement of II, using the restraints C—Cl = 1.750(5) and C—C = 1.390(5) Å and C—C—Cl = 119.0(1) and C—C(Cl)—C = 122.0(1)° (according to Wheeler & Colson, 1975; see Table 3), does not change the *wR* factor (= 0.053). The C—C distance across *m* is short [1.29(1) Å] and Cl(1)—Cl(1″) = 6.18(1) Å. It is difficult to choose a preferred model on the basis of these data. This might explain the conflicting results on the structure of the low-loaded H-ZSM-5/pdcb complex reported in the literature (see *Introduction*).

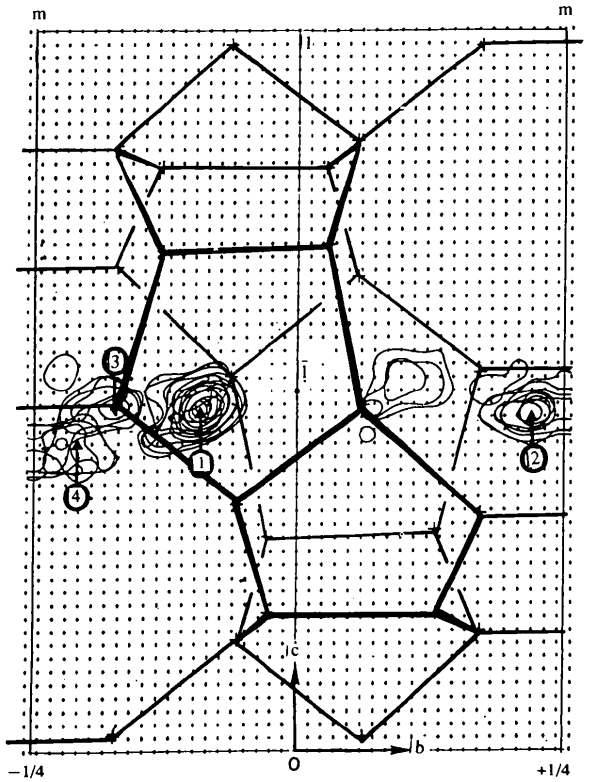

Fig. 1. Superposition of electron-density sections perpendicular to **a** at intervals of 0.0125 **a** between 0.0 ≤ **a** ≤ 0.5 of the adsorbed material in H-ZSM-5. A double 10-ring of the straight channel is indicated.

Table 2. *Results of the refinement of the two models*

	Model I	Model II
Peaks used (Fig. 1)	1, 2, 3 (or 4)	1, 2, 3, 4
Refined atoms	Cl(1), Cl(2*a*), Cl(2*b*)	Cl, C(1), C(2), C(3)
Population parameter	0.68, 0.38, 0.30	0.64 (all 4)
No. of parameters	350	353
No. of reflections	5309	5309
wR	0.053	0.053
Population parameter*		0.320 (3)
No. of parameters*		356
No. of reflections*		5306
*wR**		0.044

* Final data for a refinement using a rigid pdcb molecule.

Table 3. *Experimental geometry of p-dichlorobenzene according to Wheeler & Colson (1975; W&C) together with the simulated values (S) in an isolated pdcb molecule*

	W&C (Å)	*S* (Å)		*W&C* (°)	*S* (°)
C—C(Cl)	1.390	1.408	C—C—Cl	119.0	120.9
C—C	1.394	1.388	C—C(Cl)—C	122.0	118.2
C—Cl	1.750	1.762	C—C—C	119.0	118.9
Cl—Cl	6.243	6.360	H—C—C	120.5	118.9
C—H_{av}	1.075	1.087	H—C—C(Cl)	120.5	120.2

The final difference electron-density map for model I shows peaks (1.26 and 1.17 e Å^{-3}) around the Cl atoms, whereas for model II the map is flat and does not show any significant features at the Cl positions. In I no C atoms can be located, whereas one would expect the rotation of the pdcb molecule around the Cl—Cl axis to be considerably hindered in this section of the straight channel; the *wR* factor slightly increases during a restrained refinement. These observations indicate that, in principle, model II gives a more complete description of the electron density than model I. We therefore continued our efforts to refine II. A group refinement of a rigid pdcb molecule, using the geometry of Wheeler & Colson (1975; see Table 3) with individual isotropic displacement parameters for the C atoms and anisotropic parameters for the Cl atoms, was carried out. H atoms are added at calculated positions (C—H = 1.00 Å, C—C—H = 120.5°) and included in the group refinement. It turns out that the crystallographic mirror plane does not coincide exactly with the molecular mirror plane perpendicular to the Cl—Cl axis. The final *R*(*wR*) = 0.044(0.048) for 5306 reflections and 356 parameters. There are 2.56(2) pdcb molecules per unit cell. The final atomic parameters are given in Table 4.* The structure of the low-loaded H-ZSM-5/2.56 pdcb complex is illustrated in Fig. 2. The ranges and averaged

* List of structure factors, anisotropic thermal parameters, H-atom coordinates and complete geometry have been deposited with the IUCr (Reference: HU0426). Copies may be obtained through The Managing Editor, International Union of Crystallography, 5 Abbey Square, Chester CH1 2HU, England.

Table 4. *Fractional atomic coordinates and equivalent isotropic displacement parameters* (Å²)

$$U_{eq} = (1/3)\sum_i\sum_j U_{ij} a_i^* a_j^* \mathbf{a}_i.\mathbf{a}_j.$$

	x	y	z	U_{eq}
Si(1)	0.42283 (4)	0.05661 (6)	−0.34560 (7)	0.0119 (2)
Si(2)	0.30426 (5)	0.02861 (5)	−0.20196 (7)	0.0137 (2)
Si(3)	0.28104 (4)	0.06296 (5)	0.02023 (7)	0.0136 (3)
Si(4)	0.12323 (4)	0.06414 (5)	0.01913 (7)	0.0126 (3)
Si(5)	0.07124 (5)	0.02771 (5)	−0.19221 (7)	0.0113 (2)
Si(6)	0.18128 (4)	0.05743 (6)	−0.34191 (7)	0.0133 (2)
Si(7)	0.42151 (4)	−0.17228 (5)	−0.33321 (7)	0.0126 (3)
Si(8)	0.30404 (5)	−0.12935 (5)	−0.19323 (7)	0.0138 (2)
Si(9)	0.27404 (4)	−0.17252 (5)	0.02500 (7)	0.0130 (2)
Si(10)	0.11921 (4)	−0.17350 (5)	0.02170 (7)	0.0133 (3)
Si(11)	0.06839 (5)	−0.13023 (5)	−0.19021 (7)	0.0124 (7)
Si(12)	0.18266 (4)	−0.17263 (5)	−0.32856 (7)	0.0130 (2)
O(1)	0.3675 (1)	0.0562 (2)	−0.2609 (2)	0.0349 (9)
O(2)	0.3027 (1)	0.0632 (1)	−0.0946 (2)	0.0277 (8)
O(3)	0.2021 (1)	0.0586 (2)	0.0310 (2)	0.038 (1)
O(4)	0.1028 (1)	0.0633 (1)	−0.0960 (2)	0.0275 (9)
O(5)	0.1099 (1)	0.0531 (2)	−0.2889 (2)	0.0210 (7)
O(6)	0.2380 (1)	0.0472 (2)	−0.2602 (2)	0.039 (1)
O(7)	0.3669 (1)	−0.1599 (2)	−0.2496 (2)	0.038 (1)
O(8)	0.3047 (1)	−0.1571 (2)	−0.0824 (2)	0.0331 (9)
O(9)	0.1963 (1)	−0.1522 (1)	0.0249 (2)	0.0294 (8)
O(10)	0.0923 (1)	−0.1652 (2)	−0.0901 (2)	0.036 (1)
O(11)	0.1105 (1)	−0.1588 (2)	−0.2820 (2)	0.0274 (9)
O(12)	0.2372 (1)	−0.1512 (2)	−0.2480 (2)	0.039 (1)
O(13)	0.3093 (2)	−0.0502 (2)	−0.1920 (2)	0.056 (1)
O(14)	0.0794 (1)	−0.0514 (1)	−0.1797 (2)	0.0290 (8)
O(15)	0.4217 (1)	0.1270 (1)	−0.4037 (2)	0.0288 (9)
O(16)	0.4106 (1)	−0.0023 (2)	−0.4243 (2)	0.0302 (9)
O(17)	0.4023 (2)	−0.1329 (1)	−0.4337 (2)	0.0291 (9)
O(18)	0.1878 (1)	0.1296 (1)	−0.3928 (2)	0.0271 (8)
O(19)	0.1870 (1)	0.0003 (1)	−0.4262 (2)	0.0303 (9)
O(20)	0.1925 (2)	−0.1303 (1)	−0.4294 (2)	0.0306 (9)
O(21)	−0.0055 (1)	0.0476 (1)	−0.2048 (2)	0.0224 (8)
O(22)	−0.0086 (1)	−0.1468 (1)	−0.2093 (2)	0.0276 (9)
O(23)	0.4259 (2)	−1/4	−0.3592 (3)	0.032 (1)
O(24)	0.1902 (2)	−1/4	−0.3546 (3)	0.029 (1)
O(25)	0.2829 (2)	−1/4	0.0519 (3)	0.025 (1)
O(26)	0.1102 (2)	−1/4	0.0553 (3)	0.020 (1)
Cl(1)	0.000 (1)	0.1039 (6)	0.517 (1)	0.47 (2)
Cl(2)	−0.028 (1)	0.4162 (6)	0.521 (1)	0.156 (5)
C(1)	−0.0079 (5)	0.1915 (6)	0.5180 (7)	0.17 (2)
C(2)	−0.0551 (5)	0.2208 (7)	0.5805 (7)	0.23 (3)
C(3)	−0.0614 (5)	0.2906 (7)	0.5812 (7)	0.14 (2)
C(4)	−0.0202 (5)	0.3287 (6)	0.5196 (7)	0.11 (1)
C(5)	0.0270 (5)	0.2993 (7)	0.4571 (7)	0.082 (7)
C(6)	0.0333 (5)	0.2295 (7)	0.4563 (7)	0.108 (9)

values of d(Si—O) and ∠(Si—O—Si) in H-ZSM-5/2.56 pdcb (2.6PDCB; this report) are comparable to those in other MFI-type structures such as as-synthesized ZSM-5 containing the tetrapropylammonium ion as a template (TPAORT; van Koningsveld, van Bekkum & Jansen, 1987), the orthorhombic phase of calcined (empty) H-ZSM-5 at 358 K (HTORT; van Koningsveld, 1990), monoclinic calcined H-ZSM-5 at room temperature (MONO; van Koningsveld, Jansen & van Bekkum, 1990) and the high-loaded H-ZSM-5/8*p*-xylene complex (PARA; van Koningsveld *et al.*, 1989). The O—Si—O angle varies between 107.7 and 111.1° and averages 109.47° in each SiO_4 group. The framework geometry is compared in Table 5.

The position of pdcb at the intersection of channels might be stabilized by C—H···O contacts. The geometry of C—H···O contacts smaller than 3.70 Å is summarized in Table 6. The angle between the normal on the benzene ring plane and the positive a axis is 47.1 (3)°.

The molecular mirror plane perpendicular to the intramolecular Cl—Cl axis does not coincide with the crystallographic mirror plane. The Cl—Cl axis deviates 5.2° from [010] and is nearly parallel to (100). Therefore, there are in principle three different Cl—Cl contacts between terminal Cl atoms in neighbouring pdcb molecules in the straight channel. The contact distances between centrosymmetrically related Cl atoms are 4.16 (2) and 3.56 (2) Å. The third contact, between Cl atoms related by a twofold screw axis, is 3.81 (2) Å, in good agreement with the Cl—Cl contacts in γ-*p*-dichlorobenzene crystals [3.789 (2) and 3.800 (2) Å; Wheeler & Colson, 1975], although the packing in the latter crystal is quite different. The pdcb molecules form a chain in the straight channel. To avoid the short Cl—Cl contact of 3.56 Å the pdcb molecules in the chain might preferentially be related by a twofold screw axis, resulting in a local non-centrosymmetric structure. The 'polarity' of the chain can change after an 'empty' cross-section.

3.2. *Energy calculations*

The preferred adsorption site(s) of pdcb in H-ZSM-5 was (were) also studied by energy minimization using the software package of Biosym Technologies, San Diego, containing the Biosym CFF91 force field (Maple, Dinur & Hagler, 1988; Maple, Thacher, Dinur & Hagler, 1990), extended for zeolites by Hill & Sauer (1994). Both parts of the force field are based on quantum chemical calculations on various molecules. The parameters describing the interaction between the zeolite and the molecules (Coulomb and 6–9 Lennard-Jones terms) are taken from the separate parts of the force field without introduction of new quantum chemical or experimental data for this interaction. In Table 3 the energy optimized geometry of an isolated pdcb molecule, obtained with the CFF91 force field, is compared with the experimental geometry for a molecular crystal (Wheeler & Colson, 1975).

In a first approximation the calculations were started using fixed atomic positions for the framework and Cl atoms obtained from the X-ray analyses and four molecules of pdcb/u.c. To avoid complications of disorder around m or $\bar{1}$ the space group $Pn2_1a$ was used. As in the XRD analysis a pure silica framework (silicalite 1) was used in the calculations. The benzene ring was rotated by φ° around the Cl—Cl vector. The angle φ is approximately equal to the angle between the normal on the ring plane and the a axis (*cf.* Fig. 2). For both models the sum of the guest–host and guest–guest interaction energies (δE) was calculated. The guest–guest interaction turned out to be small (less negative than −7.54 kJ per 4 pdcb mols.). The rotational energy is presented in Fig. 3. Fig. 3 illustrates that δE is positive during rotation around

the Cl(1)—Cl(2*a*) vector (Model I*a*) as well as around the Cl(1)—Cl(2*b*) vector (Model I*b*). For Model II large regions of negative δE are calculated. The observed X-ray geometry corresponds to a minimum in δE. Thus, the calculations show that in a rigid MFI framework with the observed XRD geometry, the preferred adsorption site for the pdcb molecule is at the intersection of channels around *m*. In a next step full energy minimizations, with variable and fixed unit-cell dimensions, were performed. The complete structure (the host framework as well as the four guest molecules) was allowed to relax in $Pn2_1a$ starting from the structures corresponding to the minima in the rotation curves. Table 7 summarizes the interaction energies after relaxation using the program *Discover*-3 from Biosym Technologies (1993). For both types of optimizations (variable and fixed u.c.) the δE values for Model II are by far the lowest, again showing that the preferred adsorption sites are at the intersection of channels. These sites are mainly stabilized by the strong reduction of the repulsive term with respect to the

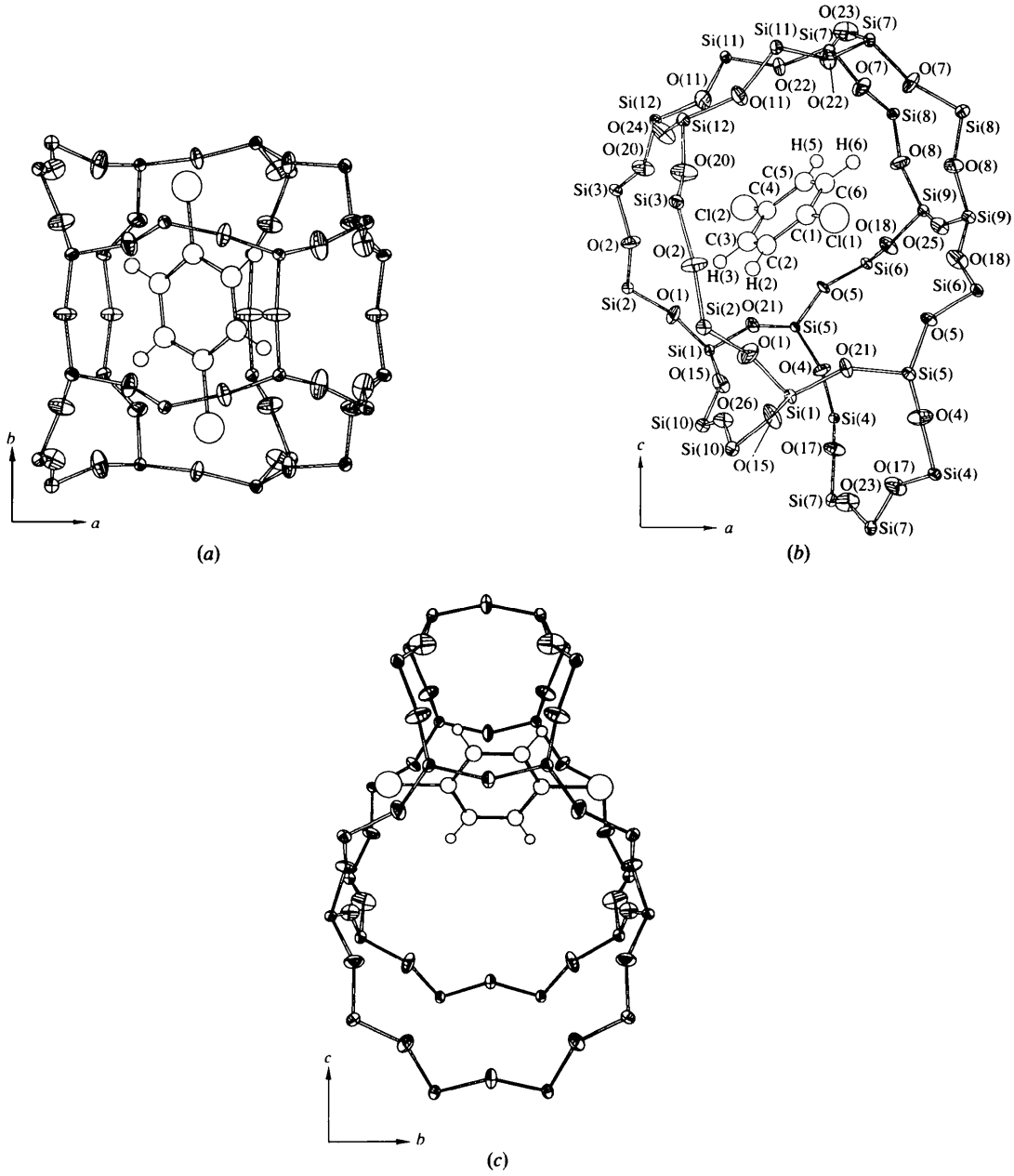

Fig. 2. *ORTEP* drawings (Johnson, 1965) of the structure of the low-loaded H-ZSM-5/2.56 pdcb complex seen (*a*) along **c**, (*b*) inclined ~ 20° along **b** and (*c*) along **a**. The atom labelling is shown in (*b*). The ellipsoids are drawn to enclose 50% probability.

Table 5. *Comparison of the framework geometry in several ZSM-5-type structures*

ZSM-5-type	Range Si—O (Å)	Range av. $Si(O)_4$ (Å)	Av. Si—O (Å)	Range Si—O—Si (°)	Range av. $Si(OSi)_4$ (°)	Av. Si—O—Si (°)
2.6PDCB	1.577–1.607 (3)	1.584–1.596	1.592	144.4–170.7 (2)	150.0–162.8	154.0
TPAORT	1.567–1.605 (4)	1.580–1.591	1.586	144.9–175.9 (4)	150.5–162.8	155.4
HTORT	1.570–1.601 (4)	1.581–1.593	1.587	145.7–177.7 (4)	150.7–163.6	155.5
MONO	1.582–1.607 (3)	1.588–1.601	1.595	141.3–169.0 (3)	147.1–158.8	153.0
PARA	1.574–1.611 (4)	1.588–1.604	1.597	138.3–172.3 (3)	148.5–162.3	154.7

Table 6. *Geometry of short p-dichlorobenzene-to-framework contacts*

(C···O < 3.70; C—H = 1.00 Å).

Contact	C···O (Å)	H···O (Å)	C—H···O (°)
C(3)—O(20^{i})	3.67 (1)	3.46 (1)	94 (1)
C(5)—O(7^{ii})	3.58 (1)	2.68 (1)	150 (1)
C(5)—O(8^{ii})	3.52 (1)	2.80 (1)	129 (1)
C(5)—O(22^{i})	3.50 (1)	2.93 (1)	117 (1)
C(6)—O(7^{iii})	3.67 (1)	2.70 (1)	163 (1)
C(6)—O(8^{iii})	3.59 (1)	2.76 (1)	140 (1)

Symmetry codes: (i) $-x, \frac{1}{2}+y, -z$; (ii) $\frac{1}{2}-x, \frac{1}{2}+y, \frac{1}{2}+z$; (iii) $\frac{1}{2}-x, -y, z+\frac{1}{2}$.

Table 7. *Sum of the host–guest and guest–guest interaction energy (δE) in kJ per unit cell in fully relaxed silicalite-1/4 pdcb complexes with $Pn2_1a$ symmetry and start-geometries corresponding to the minima (n) in the rotation curves in Fig. 3*

	Variable unit cell			Fixed unit cell		
n	*Ia*	*Ib*	II	*Ia*	*Ib*	II
1	−285.443	−254.750	−290.246	−309.149	−309.229	−323.698
2	−286.122	−256.496	−288.039	−309.011	−309.103	−325.461
3	−282.739	−258.585		−309.882	−288.496	
4	−279.008	−246.406		−294.654	−304.041	

The geometry optimizations were performed with variable and fixed unit-cell dimensions.

corresponding values in Model I calculations.* Additional information on the validity of the adsorption sites found by the minimization can be obtained by simulated annealings according to a method described by Press, Teukolsky, Vetterling & Flannery (1992). The framework atoms, with *Pnma* symmetry, were fixed at the positions obtained from the single-crystal X-ray refinement. The geometry of the pdcb molecule was kept fixed at the experimental values listed in Table 3. During the simulated annealing there were only three rotational and three translational degrees of freedom. Between the adsorbed pdcb molecules $Pn2_1a$ symmetry was preserved. In all simulations* the pdcb molecule 'jumped' to positions at the intersection of channels, regardless of its start position in the straight channel, provided that the 'start temperature' is high enough (3768 kJ mol^{-1}; comparable to the purely rotational barrier found for Model *Ib* in Fig. 3). In conclusion, full relaxations as well as simulated annealings support the result obtained by single-crystal X-ray refinement that Model II describes the most probable adsorption site.

3.3. *Orientation of p-dichlorobenzene at the intersection of channels*

At low loadings, the pdcb molecules apparently adsorb preferentially at the intersection of channels. Therefore, the discussion on the orientations of pdcb will be restricted to those obtained from the refinement of Model II. Table 8 gives the orientations of pdcb and *p*-xylene molecules at the intersection of channels in H-ZSM-5, as determined by X-ray analysis and from (full) relaxations. The orientation of the adsorbed molecule is described by the fractional coordinates (x, y, z) of its molecular centre and the angles with the positive a, b and c axes of the long molecular axis ($\alpha 1, \beta 1, \gamma 1$) and the normal on the benzene ring plane ($\alpha 2, \beta 2, \gamma 2$). The X-ray data for the *p*-xylene molecule at the intersection of channels are obtained from the analysis of PARA (van Koningsveld *et al.*, 1989). Very recently we solved the structure of the high-loaded H-ZSM-5/8 pdcb complex (= 8PDCB) by single-crystal X-ray diffraction (van Koningsveld, Jansen & van Bekkum, 1996). Preliminary results for the orientation of pdcb at the intersection have been added to Table 8. The remaining data in Table 8 are obtained

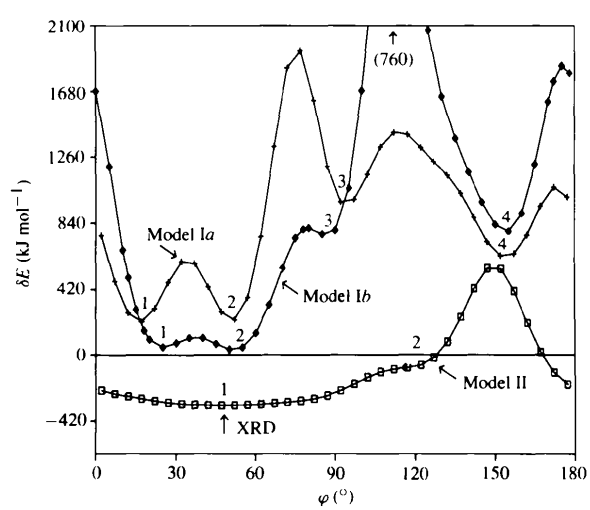

Fig. 3. Rotational energy curves for pdcb in silicate-1. The framework geometry obtained from the X-ray refinements is used. The orientation of the pdcb molecule found experimentally is indicated by 'XRD'.

*Full details are available from the authors on request.

Table 8. *Orientation of molecules adsorbed at the intersection of channels in MFI as determined by X-ray diffraction or calculated after relaxation of structures (1) and (2) (Model II) in $Pn2_1a$ with variable (var.) and fixed (fix.) unit-cell dimensions*

Angles of vectors with the positive a, b and c axes are denoted by α, β and γ, respectively ($\alpha 2$ approximately equals φ in Fig. 3). Vector 1: long molecular axis; vector 2: normal on benzene ring plane.

		X-ray		4PDCB, after relaxation			
	2.6PDCB	PARA	8PDCB	var. ← 1 → fix.		var. ← 2 → fix.	
x	0.4860	0.5105	0.5113	0.4717	0.4824	0.5177	0.4760
y	0.2400	0.2390	0.2419	0.2394	0.2403	0.2487	0.2476
z	−0.0188	−0.0188	−0.0253	−0.0167	−0.0220	−0.0396	−0.0280
$\alpha 1$	84.8	89.4	88.7	88.8	87.3	90.0	90.6
$\beta 1$	5.2	6.3	8.2	2.2	3.9	0.1	0.6
$\gamma 1$	89.6	96.3	98.1	88.2	87.2	89.9	90.2
$\alpha 2$	47.1	149.0	153.8	50.1	48.4	157.3	46.9
$\beta 2$	93.2	92.6	92.4	89.5	89.6	89.9	89.8
$\gamma 2$	136.9	−120.9	−116.1	104.1	138.4	−112.7	136.9

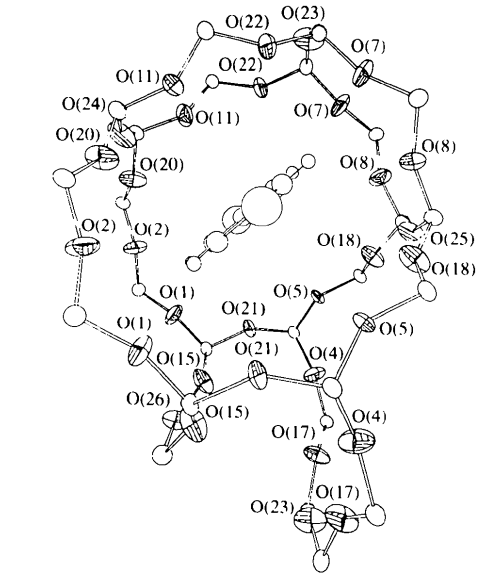

(*a*)

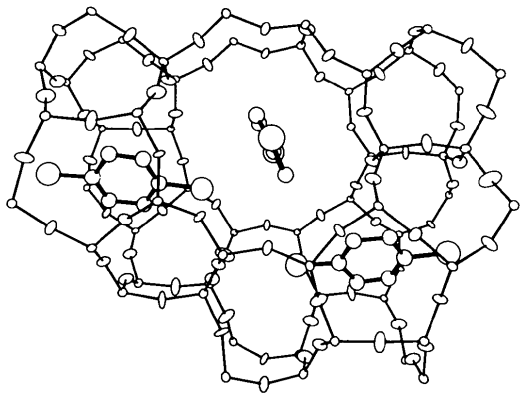

(*b*)

Fig. 4. Orientation of pdcb in (*a*) H-ZSM-5/2.56 pdcb and (*b*) H-ZSM-5/8 pdcb, corresponding to the two different rotational orientations of the relaxed structures at the intersection of channels.

after geometry optimizations of start-structures (1) and (2) in Model II (see Fig. 3). In the fixed unit-cell approximation both start-structures converge to about the same final structure. The refined orientation of the adsorbed molecule agrees perfectly with the orientation in 2.6PDCB (illustrated in Fig. 4*a*), as determined from single-crystal X-ray diffraction. With variable unit-cell dimensions structure (1) optimizes to approximately the same final structure as is obtained after refinement with fixed unit-cell dimensions. Start-structure (2), however, relaxes to a new minimum. The orientation of the pdcb molecule in this new minimum corresponds very well to the orientation of the *p*-xylene and pdcb molecule at the intersection of channels in PARA and 8PDCB, respectively. The orientation of pdcb at the intersection of channels in 8PDCB is shown in Fig. 4(*b*). The space group of PARA and 8PDCB is $P2_12_12_1$. The symmetry change from *Pnma* (for 2.6PDCB) to $P2_12_12_1$ is accompanied by significant changes (up to ±5%) in the cell dimensions. This might explain why this new minimum is only calculated using variable unit-cell dimensions.

3.4. *Pore dimensions*

Table 9 summarizes the O···O distance in 10-rings in calcined (empty) H-ZSM-5 at 358 K (HTORT) and its pdcb and *p*-xylene complexes. The influence of adsorbed material on the framework geometry is reflected by the change in pore sizes. Compared with the pores in the empty HTORT framework (*Pnma*) the straight channel pore in 2.6PDCB (*Pnma*) is strongly distorted, while the pores in the sinusoidal channel are hardly affected. In the fixed unit-cell (u.c.) approximation the deviation from *Pnma* symmetry is negligible for structure (1)* and significant for structure (2). After relaxation with variable

* The distance of the centra in the two 10-rings in the straight channel, projected along **b**, is 0.002 Å and the distances of the centra in the two 10-rings in the sinusoidal channel from $y = 0.250$ are smaller then 0.001 Å.

Table 9. *Diagonal O···O distances (Å) in 10-rings of H-ZSM-5/2.56 pdcb (2.6PDCB) with Pnma symmetry, and in silicalite-1/4 pdcb (4PDCB) calculated after relaxation in $Pn2_1a$ of both 4PDCB structures (1 and 2) of Model II with variable (var.) and fixed (fix.) unit-cell dimensions*

Pore dimensions in the empty H-ZSM-5 framework at 358 K (HTORT; *Pnma*)* and in the high-loaded complex H-ZSM-5/8*p*-xylene (PARA; $P2_12_12_1$) are added for comparison. Labelling of the O atoms is for non-centrosymmetric structures.† The labels modulus 26 correspond to those in Fig. 2. Corresponding directions in 10-rings are underlined.

		4PDCB (1)		4PDCB (2)			
	2.6PDCB	fix.	var.	fix.	var.	HTORT	PARA
Straight channel							
Ring I							
O(1)—O(33)	8.891 (4)	9.233	8.527	9.246	8.429	8.406 (6)	7.503 (2)
O(2)—O(34)	8.415	8.772	8.359	8.752	8.357	8.153	7.968
O(20)—O(44)	7.971	7.737	8.352	7.671	8.448	8.251	8.489
O(11)—O(31)	7.534	7.273	8.221	7.198	8.301	7.985	8.882
O(22)—O(47)	8.081	8.009	8.452	8.204	8.389	8.033	8.071
1/*s*‡	1.180	1.269	1.037	1.285	1.018	1.053	1.184
Ring II							
O(7)—O(27)	8.891	9.234	8.596	9.174	8.436	8.406	7.774
O(8)—O(28)	8.415	8.775	8.422	8.671	8.370	8.153	7.949
O(18)—O(46)	7.971	7.739	8.351	7.651	8.416	8.251	8.615
O(5)—O(37)	7.534	7.270	8.117	7.329	8.315	7.985	8.755
O(21)—O(48)	8.081	8.011	8.417	8.210	8.379	8.033	8.099
1/*s*‡	1.180	1.270	1.059	1.252	1.015	1.053	1.126
Sinusoidal channel							
Ring I							
O(1)—O(28)	8.002 (4)	7.813	8.398	7.664	8.368	8.077 (6)	7.578 (2)
O(2)—O(27)	8.002	7.811	8.270	7.721	8.371	8.077	8.606
O(20)—O(41)	8.292	8.213	8.423	8.118	8.383	8.308	9.071
O(24)—O(26)	8.049	8.111	8.528	8.214	8.543	8.061	8.302
O(15)—O(46)	8.292	8.212	8.369	8.184	8.383	8.308	7.456
1/*s*‡	1.036	1.051	1.031	1.072	1.021	1.031	1.217
Ring II							
O(5)—O(30)	8.062	8.177	8.449	8.417	8.360	8.042	7.447
O(4)—O(31)	8.062	8.176	8.337	8.560	8.335	8.042	8.533
O(17)—O(44)	7.954	8.037	8.263	8.074	8.257	7.945	8.846
O(23)—O(25)	8.375	8.464	8.537	8.016	8.590	8.382	8.591
O(18)—O(43)	7.954	8.038	8.236	8.068	8.247	7.945	7.283
1/*s*‡	1.053	1.053	1.037	1.068	1.042	1.056	1.215

* Pore dimensions in the empty zeolite, calculated after (full) relaxation of the framework, are available from the authors on request. † One of the possible ways to calculate the 'diagonal' O···O distances in 2.6PDCB is deposited as supplementary data to Table 9. ‡ 1/*s*: ratio of longest and shortest pore dimensions.

u.c. dimensions the differences in pore dimensions, zero by symmetry in *Pnma*, are large in both structures. This might indicate that, given the observed u.c. dimensions, structure (1) represents the most probable adsorption configuration in low-loaded silicate-1/pdcb systems (hereafter termed 4PDCB).

The calculated values of the pore sizes in 4PDCB are rather different from the experimental values in 2.6PDCB. The pores in the fixed u.c. structures are deformed to a more elliptical form than in the variable u.c. structures; the observed windows in 2.6PDCB are just in between (compare the 1/*s* values in Table 9). The differences are most pronounced for the straight channel windows.

Table 9 shows that the straight channel pore in HTORT is cloverlike with two 'long' O···O distances: O(1)—O(7) and O(20)—O(18). The same pore form is calculated after relaxation of structure (2) with variable u.c. dimensions. The long O(1)—O(7) direction in HTORT corresponds to the direction of the short molecular axis of the pdcb molecule (and the longest pore dimension) in the adsorption site in 2.6PDCB, as well as in three of the four relaxed 4PDCB structures. The long O(20)—O(18) direction deviates only 10° from the direction of the short molecular axis of the pdcb molecule in the fourth relaxed structure (structure 2; var. u.c.) and of the *p*-xylene and pdcb molecule at the intersections of channels in high-loaded PARA and 8PDCB, respectively (see also Table 8). The shortest (largest) pore dimension in HTORT becomes the largest (shortest) in the high-loaded complexes.

In the double 10-ring in the sinusoidal channel of HTORT, 2.6PDCB and both 4PDCB structures (fixed u.c.) the long dimension of the one 10-ring is in the same direction as the short dimension in the adjacent 10-ring, resulting in a more circular effective double 10-ring pore. The sinusoidal channel is therefore less accessible for adsorption of pdcb (or *p*-xylene) than the straight channel. However, in the relaxed structures with variable u.c. the maximum pore sizes in both 10-rings are in the same direction and, in principle, the pdcb (*p*-xylene) molecule can enter the sinusoidal channel much easier. This is in agreement with the pore-form of the 10-rings in the sinusoidal channel observed in PARA.

In structure (2) (var. u.c.) the orientation of pdcb agrees with the *p*-xylene and pdcb molecules at the

intersection of channels in the high-loaded PARA and 8PDCB complexes (see Table 8 and Fig. 4). The other independent molecule in the high-loaded adducts is accommodated in the sinusoidal channel. It appears that adsorption of a first molecule in the O(20)—O(18) direction in the straight channel promotes the adsorption of a second molecule in the sinusoidal channel, provided the unit-cell dimensions can change.

4. Concluding remarks

Single-crystal X-ray diffraction, simulated annealing calculations and force-field calculations show that the favourable adsorption site for *p*-dichlorobenzene (pdcb) in H-ZSM-5, at loadings up to 4 molecules per u.c., is at the intersection of channels. In nearly all calculations the orientation of the relaxed molecule is very close to the orientation found from the X-ray analysis. A second rotational position at the intersection is found from calculations where the unit-cell dimensions are allowed to change. It appears that the deformations of the straight and sinusoidal channel are correlated in such a way that adsorption of a molecule in this 'second' position at the intersection of channels enhances the accessibility of the sinusoidal channel for adsorption of another molecule. In high-loaded H-ZSM-5/8*p*-xylene the *p*-xylene molecule at the intersection of channels indeed occupies this second position. The same situation is found very recently in the high-loaded H-ZSM-5/8pdcb complex (van Koningsveld *et al.*, 1996).

We thank Professor H. van Bekkum for his interest and encouragement of this work.

References

Biosym Technologies (1993). *Biosym Catalysis and Sorption Software*. Version 3. Biosym Technologies, San Diego.

Gies, H., Marler, B., Fyfe, C. A., Kokotailo, G. T., Feng, Y. & Cox, D. E. (1991). *J. Phys. Chem. Solids*, **52**, 1235–1241.

Hall, S. R., Flack, H. D. & Stewart, J. M. (1992). Editors. *Xtal3.2 Reference Manual*. Universities of Western Australia, Australia, Geneva, Switzerland, and Maryland, USA.

Hill, J.-R. & Sauer, J. (1994). *J. Phys. Chem.* **98**, 1238–1244.

Johnson, C. K. (1965). *ORTEP*. Report ORNL-3794, revised June 1970. Oak Ridge National Laboratory, Tennessee, USA.

Koningsveld, H. van (1990). *Acta Cryst.* B**46**, 731–735.

Koningsveld, H. van, van Bekkum, H. & Jansen, J. C. (1987). *Acta Cryst.* B**43**, 127–132.

Koningsveld, H. van, Jansen, J. C. & van Bekkum, H. (1987). *Zeolites*, **7**, 564–568.

Koningsveld, H. van, Jansen, J. C. & van Bekkum, H. (1990). *Zeolites*, **10**, 235–242.

Koningsveld, H. van, Jansen, J. C. & van Bekkum, H. (1992). *Extended Abstracts of the 9th International Zeolite Conference*, Montreal, 5–10 July 1992, Abstract RP201, Butterworth, USA.

Koningsveld, H. van, Jansen, J. C. & van Bekkum, H. (1996). *Acta Cryst.* B**52**, 140–144.

Koningsveld, H. van, Tuinstra, F., van Bekkum, H. & Jansen, J. C. (1989). *Acta Cryst.* B**45**, 423–431.

Maple, J. R., Dinur, U. & Hagler, A. T. (1988). *Proc. Natl Acad. Sci. USA*, **85**, 5350–5354.

Maple, J. R., Thacher, T. S., Dinur, U. & Hagler, A. T. (1990). *Chem. Des. Autom. News*, **5**, 5–10.

Mentzen, B. F. & Sacerdote-Peronnet, M. (1993). *Mat. Res. Bull.* **28**, 1161–1168.

Press, W. H., Teukolsky, S. A., Vetterling, W. T. & Flannery, B. P. (1992). *Numerical Recipes in C*, 2nd edn. Cambridge University Press.

Wheeler, G. L. & Colson, S. D. (1975). *Acta Cryst.* B**31**, 911–913.